J Solid State Electrochem (2007) 11: 259–266
DOI 10.1007/s10008-006-0102-6

ORIGINAL PAPER

L. M. M. dos Santos · M. M. Lemos Salta · I. T. E. Fonseca

The electrochemical behaviour of bronze in synthetic seawater

Received: 28 November 2005 / Revised: 18 January 2006 / Accepted: 20 January 2006 / Published online: 21 March 2006

Abstract This paper reports a voltammetric study of bronze in synthetic seawater (SSW). The effects of buffering and deoxygenating were particularly visible in the transpassive region. The breakdown of the anodic passive film on bronze leads to a well-defined activation peak in the transpassive region typical of a nucleation and growth of pits. The breakdown potential of the passivity was shown to vary with the experimental conditions, namely, with buffering and deoxygenating. Buffering has shown to lead to more stable passive films and deoxygenating to higher oxidation currents. Scanning electron microscopy with energy dispersive spectrometer (SEM/EDS) studies of bronze samples with 1-month exposure in non-deoxygenated buffered and non-buffered SSW under open circuit potential have shown significant differences in their morphology: a uniformly cracked surface and a surface showing large and spherical precipitates of about 50 μm uniformly distributed along the surface, respectively, for bronze coupons in buffered (pH 9) and in non-buffered SSW. The EDS technique has identified Cu, O, Cl and Na on the corrosion products of bronze in non-buffered SSW, whilst in buffered media, Sn was also identified. In non-buffered media, open circuit potentials have shown to be all the time less negative than in the buffered media. After 1-month exposure the E_{OCP} of bronze samples in both media seem to converge to −0.131 and −0.155 V vs Ag|AgCl, respectively. This potential can be assigned to the formation of cuprite, Cu_2O and nantokite, CuCl. The analysis of the SEM images after the removal of the corrosion products has shown descuprification with higher intensity on the surface from coupons in non-buffered SSW.

Keywords Bronze · Synthetic seawater (SSW) · Breakdown of passivity · Buffering · Deoxygenating

L. M. M. dos Santos · I. T. E. Fonseca (✉)
Departamento de Química e Bioquímica,
Faculdade de Ciências,
Universidade de Lisboa, CECUL,
R. Ernesto Vasconcelos, Ed. C8,
1749-016 Lisboa, Portugal
e-mail: itfonseca@fc.ul.pt
Tel.: +351-217500904
Fax: +351-217500892

M. M. Lemos Salta
Laboratório Nacional de Engenharia Civil,
Av. do Brasil, 101,
1700-066 Lisboa, Portugal

Introduction

Copper and copper alloys are very often used in marine environments. On the other hand, there is a great interest in the study of ancient and historical bronzes (Cu–13Sn alloys) covered with natural patinas grown on artefacts exposed for long periods to soil, atmosphere, circulating waters and seawater (see Robbiola et al. [1] and references therein).

The corrosion, passivation and breakdown of passivation of copper in the presence of aggressive anions, i.e. Cl^-, HCO_3^-, SO_4^{2-}, NO_3^-, have been investigated by many authors (2–14 and references therein). It has been demonstrated that the passive layer on copper in chloride aqueous solution is composed by copper oxides and copper chlorides, although complex ions may also be formed, i.e. $CuCl_2^-$ and $CuCl_3^-$, depending on the pH and chloride concentration.

Duthil et al. [11] in a study of copper in chloride-sulphate containing solutions have observed pit morphology depending on the relative concentration of both anions. Edwards et al. [12], among others, have concluded that the aggressiveness of one species towards the corrosion of copper or copper alloys can be modified by the presence of other species. However, as remarked by those authors, the synergetic effect of various anions remains unclear and deserves further studies to understand the electrochemical behaviour of pure metals and alloys in real water systems, namely in seawater. A systematic voltammetric study of copper in synthetic seawater was performed by our group [13].

Studies on bronze alloys in chloride media have been undertaken by Sutter and co-workers [15–17] and also by Souissi et al. [18], among others.

Ammeloot et al. [16] have found selective dissolution of copper in the Cu–13Sn alloy in chloride media leading to an oxide layer enriched in tin. They also have observed cracking corrosion.

Mansfeld and Little [19] have reported higher corrosion rates for copper in natural seawater in comparison with synthetic seawater.

Cyclic voltammetry proved to be a powerful technique for mechanistic and kinetic studies of metals and alloys and also to investigate the influence of various parameters, such as temperature, pH, dissolved O_2, buffering, etc.

This paper reports data from a voltammetric study on the corrosion, passivation and breakdown of passivity of bronze in deoxygenated and non-deoxygenated, buffered and non-buffered synthetic seawater. It is intended to pursue parallel electrochemical studies with bronze in natural seawater, where the effects of microbiological induced corrosion certainly play their role.

Experimental details

Working electrodes were made from a bronze rod with the chemical composition given in Table 1.

A three-electrode, two-compartment cell was used for cyclic voltammetric studies. The secondary electrode was a platinum foil and the reference electrode was a commercial silver/silver chloride electrode (Ag | AgCl, KCl 3 M) connected to the main compartment of the cell by a Luggin capillary. The working electrode, a disc with a geometric area of 0.196 cm^2, was mechanically polished with alumina powder down to 0.05 μm, then rinsed several times with distilled water and finally dried with acetone. Before each voltammetric experiment, the bronze electrode was polarised for 15 s at −1.300 V vs Ag|AgCl. Dissolved O_2 was removed by bubbling N_2 from L' Air Liquid.

A synthetic seawater solution (3% in Sea Salts from Sigma) was prepared with deionised Milli-Q water from Millipore. Thus, the composition of synthetic seawater solution is the following: 0.4 M Cl^- + 0.02 M SO_4^{2-} + 0.04 M Mg^{2+} + 0.35 M Na^+ + 0.008 M K^+ + 0.007 M Ca^{2+} + 0.025 M CO_3^{2-}/HCO_3^- + minor amounts of Br^-, I^-, F^- and Li^+. Buffered solutions of pH 9.0 have been prepared with borax (0.025 M $Na_2B_4O_7$).

Cyclic voltammetric studies were performed via a modular automated acquisition system Autolab (Eco chemie B. V.) composed by a Potentiostat PSAST 10, a digital/analogic converter, DAC124 and an analogical/digital converter, ADC 124, connected to a personal computer equipped with an appropriate programme (GPES) for data acquisition.

Table 1 Chemical composition of the bronze alloys

Element	Cu	Sn	Zn	Pb	P	Ni
Percentage	88.0	11.2	0.2	0.19	0.19	0.08

Scanning electron microscopy with energy dispersive spectrometer (SEM/EDS) studies of bronze samples exposed in buffered and non-buffered seawater with and without the corrosion products were performed with a scanning electron microscope JEOL, model JSM-6400. Whenever it was found important, EDS spectra were recorded with an X-ray diffractometer Oxford instruments, model Inca x sight. The corrosion products were removed by dipping the specimens for 5 to 10 s in a solution made with sulphuric acid and potassium dichromate, according to ISO/DIS 8407.3 [20].

Results and discussion

Cyclic voltammetric studies

Cyclic voltamograms, CVs, from bronze polarised between −1.300 and +0.200 V at 50 mV s^{-1} in non-deoxygenated and deoxygenated, non-buffered solutions of SSW are given in Fig. 1. Data clearly show the effects of dissolved O_2. Differences are particularly visible in the transpassive region, i.e. at $E_{\lambda a} > -0.100$ V, where $E_{\lambda a}$ means the reverse anodic potential. In deoxygenated media, the pair of peaks A_{III}/C_{III}, with a shape typical of a new phase formation, is well-defined. Peaks A_{III} and C_{III} appear at +0.082 and −0.160 V, with intensities of 4.27 and 1.88 mA cm^{-2}, respectively. The charges associated with these peaks are quite high (9.1 and 3.8 mC cm^{-2}, respectively); however, the charge of peak C_{III} is only about one-third of peak A_{III}, indicating that not all the oxidised species formed at peak A_{III} have been reduced at peak C_{III}.

The corresponding pair of peaks is not so well-defined in non-deoxygenated media. A broad anodic peak is visible at +0.070 V with a peak current density of 0.67 mA cm^{-2} and the corresponding cathodic peak, C_{III}, with an intensity

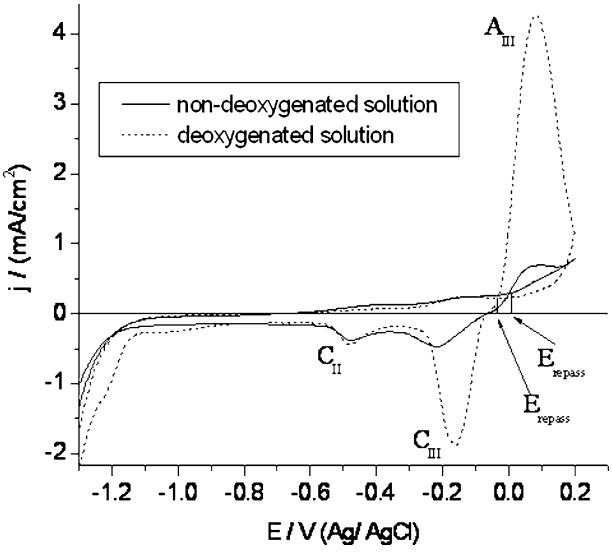

Fig. 1 CVs of bronze samples in non-buffered SSW. *Solid line* non-deoxygenated, *broken line* deoxygenated. $E_{\lambda a}$ = +0.200 V. ν = 0.050 V s^{-1}

of 0.47 mA cm^{-2} appears at −0.217 V. The observed behaviour at high anodic potentials is characteristic of the dissolution of the substrate and/or of the compounds, i.e. $CuCl_2$, which leads to a poor protection of the anodic oxides/chlorides against corrosion at high anodic potentials.

During the anodic polarisation of bronze in synthetic seawater (a solution of 0.4 M in Cl^- and 0.02 M in SO_4^{2-}), compounds such as copper oxides or hydroxides, alkali copper chlorides and copper sulphates may be formed by electrochemical and/or chemical reactions, i.e.

$$Sn + 2H_2O \rightarrow SnO_2 + 4H^+ + 4e^- \quad (1)$$

$$Cu + 2H_2O \rightarrow CuO_2 + 4H^+ + 4e^- \quad (2)$$

$$Cu + H_2O \rightarrow CuO + 2H^+ + 2e^- \quad (3)$$

$$Cu + Cl^- \rightarrow CuCl + e^- \quad (4)$$

$$Cu + 2Cl^- \rightarrow CuCl_2 + 2e^- \quad (5)$$

$$Cu_2O + Cl^- + 2H_2O \rightarrow Cu_2(OH)_3Cl + H^+ + e^- \quad (6)$$

$$4Cu + SO_4^{2-} + 6H_2O \rightarrow CuSO_4 \cdot 3Cu(OH)_2 + 6H^+ + 8e^- \quad (7)$$

$$4CuO + SO_4^{2-} + 2H_2O + 2H^+ \rightarrow CuSO_4.3Cu(OH)_2 \quad (8)$$

In the presence of high concentrations of Cl^-, cuprous complexes, i.e. $CuCl_2^-$, may be formed according to the reaction:

$$CuCl + Cl^- \rightarrow CuCl_2^- \quad (9)$$

On the other hand, it is well-known that SnO_2 is insoluble in slightly alkaline medium, even in the presence of complexing agents; thus, the soluble species would not involve Sn.

In the transpassive region, when pitting occurs, the attack of the bulk copper under the pits may occur leading to complexes or non-complexes Cu^{2+} species, depending on the chloride concentration and local pH. The dissolution of the substrate and/or of the compounds, i.e. $CuCl_2$, may occur through reactions,

$$Cu + 2Cl^- \gamma\ CuCl^{2-} \quad (10)$$

$$Cu^+ \rightarrow Cu^{2+} + e^- \quad (11)$$

$$CuCl_2 + Cl^- \rightarrow CuCl_3^- \quad (12)$$

Figure 2 presents CVs from bronze and copper electrodes in synthetic seawater recorded under identical experimental conditions.

The CVs from bronze show higher charges under the well-defined peaks, A_{III}/C_{III}, in the transpassive region. Peak A_{III} at +0.082 V with a peak current density of 4.27 mA cm^{-2} and peak C_{III} at −0.162 V with a current density of 1.88 mA cm^{-2}. The charge under the anodic reactivation peak is of the order 9.1 mC cm^{-2} and that of the corresponding cathodic peak is 3.8 mC cm^{-2}. The repassivation potential of bronze is −0.030 V. Extending the anodic polarisation potential to +0.400 V for bronze in deoxygenated non-buffered SSW (see Fig. 3), two additional cathodic peaks, peaks C_{IV} and C_V, located at −1.001 and −1.205 V, respectively, near the hydrogen evolution region, are observed during the cathodic cycle. A peak similar to peak C_{IV} has been observed by other authors, namely by Souto et al. [14], for Cu polarised at 10 mV s^{-1}, in a solution 0.002 M NaOH + 1 M Na_2SO_4. On the other hand, a peak identical to peak C_V has been observed by Díaz et al. [21] in a voltammetric study of Sn in a borate buffer solution. These two peaks observed on bronze may then be attributed to the reduction of soluble Cu(I) species to Cu(0) and of SnO_2 to Sn(0), respectively.

As it can be observed in Fig. 3, peaks C_{IV} and C_V were observed only at low scan rates. This behaviour indicates that the corresponding electrochemical processes present slow kinetics.

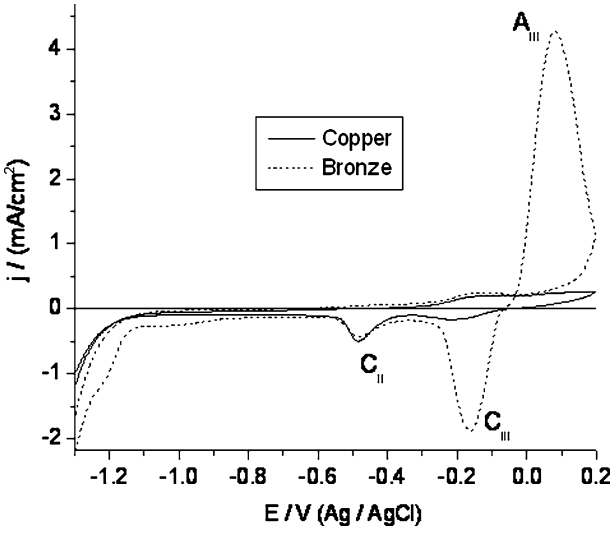

Fig. 2 CVs of bronze (*broken line*) and copper (*solid line*) samples in deoxygenated, non-buffered SSW. $E_{\lambda a} = +0.200$ V·ν=50 mV s^{-1}

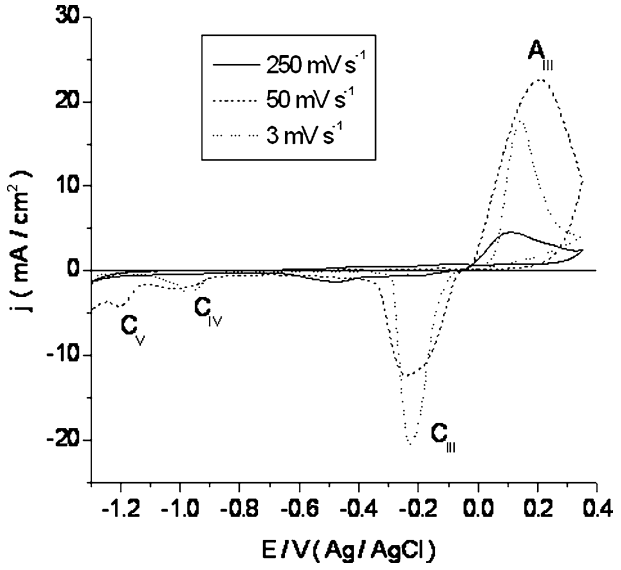

Fig. 3 CVs of bronze in deoxygenated, non-buffered SSW. $E_{\lambda a} = +0.350$ V. Sweep rates as indicated

Figure 4 shows the effects of buffering. It is clearly shown that buffering, pH 9, contributes to a displacement of the breakdown of passivity in the positive direction. Whilst in non-buffered media the reactivation peak, A_{III}, is already observed at +0.082 V, the current plateau associated with the passivation of bronze in buffered media remains stable, at least till +0.200 V. The small cathodic peak C_{II}, with a peak current density of 0.45 mA cm^{-2}, appears earlier in buffered media (Ep^{CII}=−0.397 V against −0.433 V in the non-buffered media). Thus, data indicate that buffering contributes to maintain the passive film stable, at least for polarisations until +0.200 V.

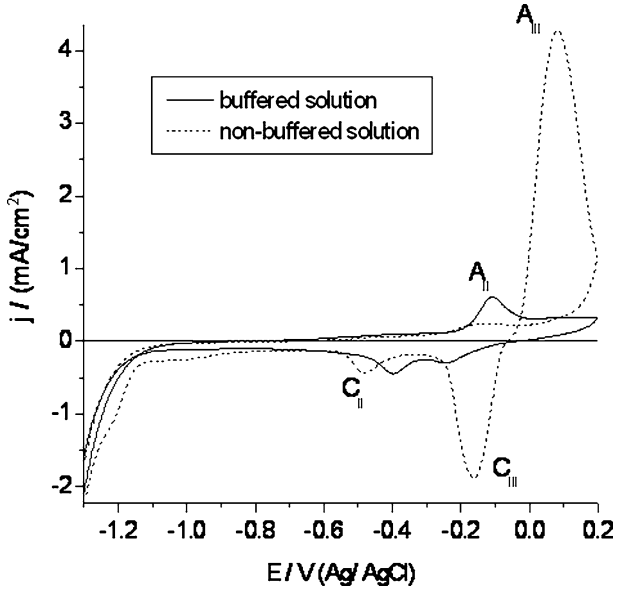

Fig. 4 CVs of bronze in deoxygenated: (*solid line*) buffered, pH=9.0; (*broken line*) non-buffered SSW $E_{\lambda a} = +0.200$ V. ν=50 mV s^{-1}

Others experiments have shown that buffering, pH 9, shifts the breakdown of passivity of bronze in synthetic seawater to much more positive values (see data in Fig. 5).

Data of Fig. 5 show that in buffered media, the breakdown of the passivity occurs at $E_{\lambda a} \cong +0.400$ V. Ferreira et al. [13] have also observed a similar behaviour for copper in synthetic seawater. A displacement of the repassivation potential from +0.120 to +0.460 V vs saturated calomel electrode due to the effect of buffering was observed in that study.

The total anodic, Q_a^t, and cathodic, Q_c^t, charges under the CVs of Figs. 1, 2 and 4 for polarisations from −1.300 to + 0.200 V vs Ag|AgCl are reported in Table 2, as well as the breakdown potentials.

Data on Table 2 allow the following conclusions:

1. Deoxygenating leads to an increase of the total anodic and cathodic charges. The ratio $\left(Q_a^t/Q_c^t\right)$ changes from 0.5 to 1.3. In the presence of O_2, the current due to oxygen reduction contributes to the total cathodic current, leading to a value of $\left(Q_a^t/Q_c^t\right) << 1$. In the absence of dissolved O_2, a shift of the breakdown potential from +0.010 to +0.160 V is observed, which means that the passive film is more stable in the absence of O_2.
2. A comparison between the total anodic and cathodic charges on the CVs from bronze and copper show that polarisation of bronze leads to much higher charges. On the other hand, the ratio $\left(Q_a^t/Q_c^t\right)$ shows a decrease from 1.3 to 0.6, indicating that the presence of tin, as the major additive to copper in the bronze alloy, contributes to an increase of the amount of soluble species. On the other hand, data show also that the passive film of bronze presents a much lower resistance to the breakdown of passivity when compared with pure copper ($(E_b = +0.160$ V against + 0.380 V).

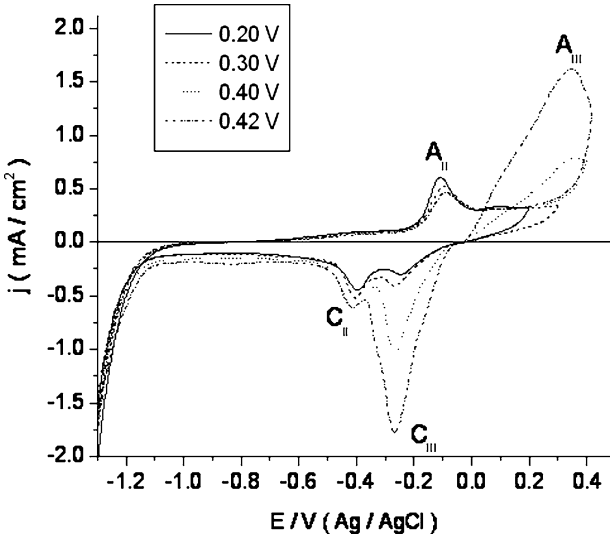

Fig. 5 CVs of bronze in deoxygenated buffered SSW, pH=9.0. $E_{\lambda a} = +0.2, +0.3, +0.4$ and +0.420 V. ν=50 mV s^{-1}

Table 2 Electrochemical data measured on the CVs of Figs. 1, 2 and 4

System	Q_a^t / Q_c^t (mC cm^{-2})		Q_a^t /Q_c^t	E_b (V vs Ag|AgCl)
bronze|non-buffered non-deox$^+$. SSW* (−1.300 to 0.200 V)	2.2	4.4	0.5	0.010
bronze|non-buffered deox$^+$-SSW* (−1.300 to 0.200 V)	12	8.7	1.3	0.160
copper|non-buffered deox.$^+$ SSW* (−1.300 to 0.400 V)	1.5	2.4	0.6	0.380
bronze|buffered deox$^+$. SSW* (−1.300 to 0.400 V)	3.2	3.4	0.9	0.340

SSW*Synthetic seawater, *deox*$^+$ deoxygenated

3. Buffering the deoxygenated synthetic seawater leads to much lower total anodic and cathodic charges and to changes in the ratio $\left(Q_a^t/Q_c^t\right)$ from 1.3 to 0.9, indicating that in non-buffered media, the amount of soluble species is much higher than in buffered media. Buffering contributes also to shift the breakdown potential to more anodic values (i.e. from +0.160 V to + 0.340 V).

In effect, deoxygenating and buffering both contribute to a displacement of the breakdown potential of the passive bronze into the anodic direction. With regard to the charges, deoxygenating leads to much higher charges, whilst buffering acts in a reverse way leading to much lower oxidation charges.

Electrochemical reduction spectra

Figure 6 presents the electrochemical reduction spectra of a bronze sample polarised potentiodynamically at 0.020 V s^{-1} in a deoxygenated non-buffered solution of SSW and then kept under potentiostatic polarisation at 0.0001 V for 1, 2 and 5 min, respectively. Peak C_{III}, which has been assigned to the reduction of Cu(II) compounds, i.e. CuO/$Cu(OH)_2$ and/or $CuCl_2$, is seen to increase with the holding time at the anodic polarisation potential, as well as peak C_{IV}. This peak may be attributed to the reduction of Cu(I) species to Cu (0), whilst the peak C_V, due probably to the reduction of SnO_2 to Sn (0), has an opposite behaviour. This means that the holding time has generally led to an increase of the thickness of the film at the bronze surface.

Bronze under open circuit potential

Figure 7 gives the open circuit potential curves, E_{OCP} vs time, of bronze samples immersed in non-deoxygenated buffered and non-buffered SSW, over a period of 30 days. Data show that in buffered media, the E_{OCP} starts at −0.180 V and reaches a maximum displacement of −0.130 V, after ca 2 days. It is then displaced abruptly again in the cathodic direction, reaching the value of about −0.16 V after 1 month. In non-buffered media, the E_{OCP} are always less negative than in the buffered media. Larger displacements are observed during longer periods, i.e. during the first week, from −0.217 to −0.084 V. Then over

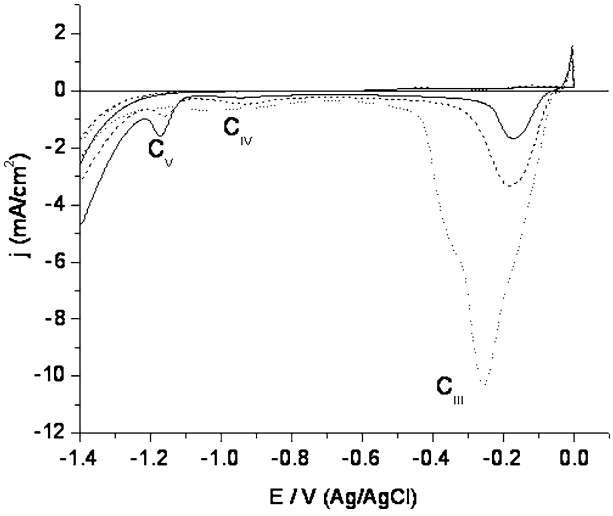

Fig. 6 Electrochemical reduction spectra from a bronze sample polarised potentiodynamically from − 1.400 V to 0.000 V and then kept under potentiostatic polarisation at 0.001 V, in deoxygenated non-buffered SSW during (*solid line*) 1 min, (*broken line*) 2 min and (*dotted line*) 5 min. ν=0.020 V s^{-1}

the next 3 weeks, the potential suffers a displacement in the negative direction reaching a value around. According to the literature [16], those potential can be assigned to the formation of cuprite, Cu_2O, and/or nantokite, CuCl. A great number of regular and periodic oscillations are observed on the E_{OCP} curves of bronze, particularly in the non-buffered SSW.It is worthwhile to notice that thermodynamic data of Fig. 7, when compared with the Pourbaix diagrams, allow the proposal of Cu_2O and CuCl as possible compounds formed on bronze surfaces after a 1-month immersion in SSW.

Visual observation of bronze samples with 1-month of exposure in SSW show the formation of a thin, slightly red film covering the total surface on both samples, possibly cuprite, Cu_2O, and also white precipitates, possibly SnO_2. It was also observed that the surface of the sample immersed in the non-buffered SSW solution present more amounts of greenish products (possible chloride salts, i.e. atacamite, paratacamite and/or botalkite).

The electrochemical reduction spectra of the corrosion products on bronze coupons, with 1-month of exposure at open circuit potential in a non-deoxygenated, non-buffered and buffered SSW solution, are given in Fig. 8. The reduction spectra show only one peak located nearly at −1.400 V.

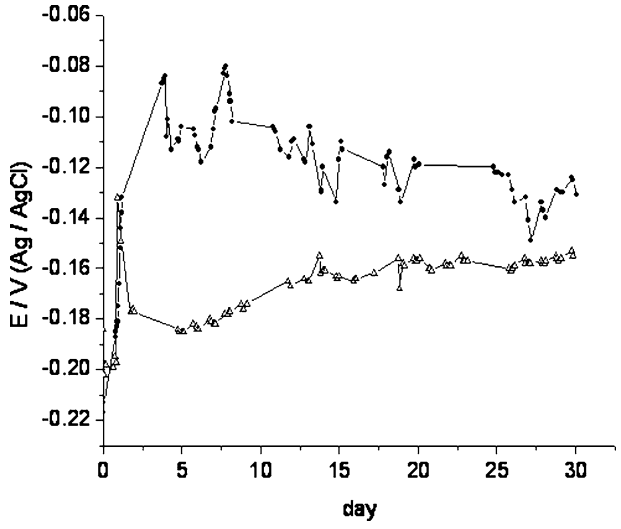

Fig. 7 E_{OCP} vs time curves of bronze samples immersed over 30 days in non-deoxygenated solutions of SSW (— Δ —) buffered and (— ● —) non-buffered

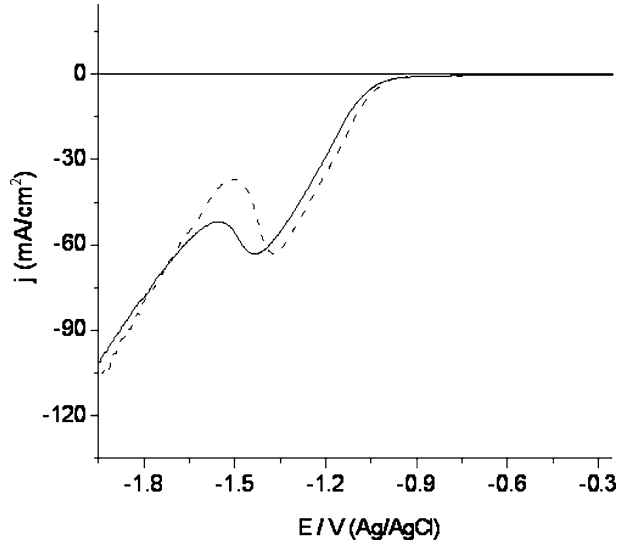

Fig. 8 Electrochemical reduction spectra from a bronze sample kept at open-circuit potential in non-deoxygenated: (*broken line*) buffered, (*straight line*) non-buffered SSW solutions for 1 month. ν=0.020 V s^{-1}

Scanning electron microscopy with energy dispersive spectrometer studies

The surface morphology of bronze samples with 1-month of exposure at open circuit potential in buffered and non-buffered solutions of SSW has been observed by scanning electron microscopy. Figure 9 shows SEM images and EDS spectra of particular zones of bronze samples with 1-month of immersion in non-deoxygenated buffered and non-buffered SSW, before the removal of the corrosion products.

Under similar amplifications, the images of the bronze samples, with 1-month of exposure in buffered and non-buffered SSW, show significant differences: a uniform layer of corrosion products on the bronze surface immersed in the buffered media with the EDS spectra revealing the presence of Cu, O, Sn, Na, Ca and Mg indicates that this layer is mainly a mix of copper oxides and tin oxides and, possibly, minor amounts of sodium chloride and sodium or calcium carbonates. The white lines on the SEM image with a distribution type cracking correspond to the formation of corrosion products more rich in tin oxide. The surface of the corresponding samples immersed in the non-buffered solution of SSW shows spherical zones of localised corrosion with precipitates of about 50 μm, almost uniformly distributed over the entire surface. These precipitates are mainly composed of copper oxides, copper and/or sodium chlorides, since the EDS spectra of zone B identifies Cu, O, Na and Cl.

According to the literature [21], the corrosion compounds on bronze alloys in chloride media are mainly copper basic compounds or a mixture of copper and tin oxides compounds. In neutral or near neutral chloride media, SnO_2 is insoluble whilst Cu_2O can dissolve in the electrolyte as $CuCl_2^-$. The solubility of SnO_2 goes through a minimum at pH 8.5. Photoelectrochemical studies performed in non-deoxygenated 0.5 M NaCl aqueous solutions by Ammeloot et al. [16] have evidenced the simultaneous presence of SnO_2 and CuO_2, with the ratio between these two oxides depending on the immersion time.

Debiemme-Chouvy et al. [15], from a XPS study of bronze samples exposed in 0.5 M NaCl aqueous solution, have concluded that after 21 h of exposure the composition of the outer layer is rich in SnO_2 whilst after 36 h is mainly composed by Cu_2O. From SEM/EDS data, Debiemme-Chouvy et al. [15] have concluded that bronze samples corresponding to higher times of exposure, i.e. 48 h, in a stagnant, non-deoxygenated, near-neutral 0.5 M NaCl aqueous solution show a heterogeneous structure with 50-μm wide zones rich in tin in a matrix rich in copper. The selective dissolution of copper was confirmed whilst SnO_2 remains on the surface. According to those authors, copper ions then diffuse along the SnO_2 layer leading to Cu_2O covering progressively the thin SnO_2 film.

Figure 10 shows the SEM images and the EDS spectra of the bronze surfaces reported in Fig. 9 after the removal of the corrosion products (probably not completely removed). Figure 10a shows still a few zones (zone C) of spherical shape with a diameter of about 130 μm for which the EDS spectra identifies Cu, Cl, Sn and O. The entire surface shows an almost uniform pattern with few pits (black spots), whilst Fig. 10b shows a pattern that may be related with the selective dissolution of Cu, i.e. the so-called decuprification process.

Conclusions

1. Deoxygenating leads to significant differences on the polarisation curves (CVs) of bronze samples in SSW, particularly in the transpassive region: a well-defined anodic peak, A_{III}, at 0.082 V following the breakdown of the passive film is visible. Its charge is 9 mC cm^{-2}, whilst in non-deoxygenated media, it is only 0.5 mC

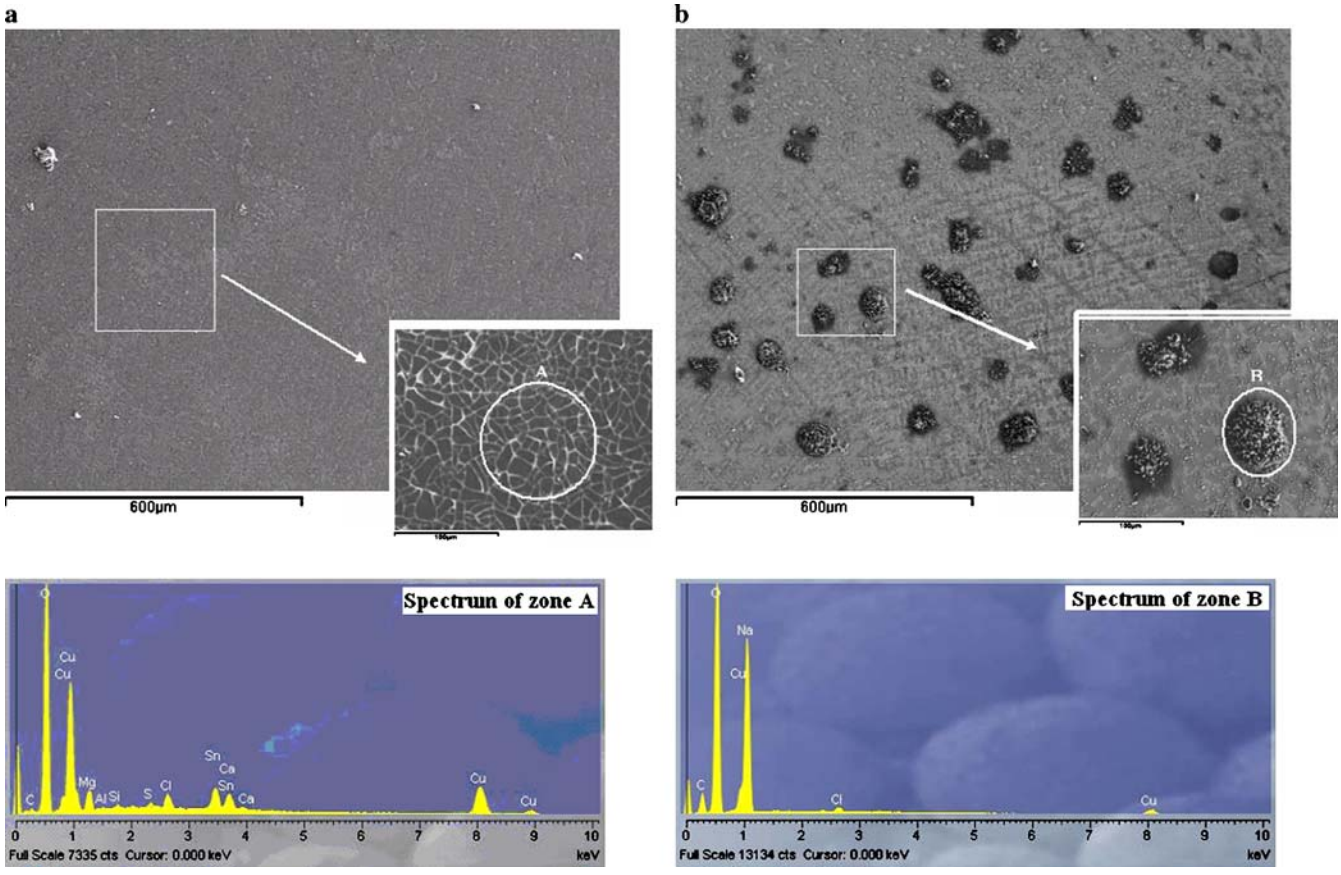

Fig. 9 SEM images and the corresponding EDS spectra from bronze coupons with 1-month of exposure in non-deoxygenated solutions of SSW, before the removal of the corrosion products: **a** buffered, **b** non-buffered media

cm^{-2}. The amount of soluble species is higher, in deoxygenated SSW, since, $Q_a^t >> Q_c^t$. Therefore, deoxygenating leads to a more stable film.

2. The breakdown of the passivity in deoxygenated, non-buffered media occurs easier and at much higher rates on passive bronze than on copper.
3. Buffering the SSW, pH 9, contributes to an increase in the stability of the passive film on bronze, which remains stable, at least until +0.200 V. However the charges involved in the transpassive corrosion process (Q_{AIII}=9.1 mC cm^{-2} and Q_{CIII}=3.8 mC cm^{-2}) are quite high. The ratio between the anodic and cathodic charges decreases, indicating that buffering contributes, as expected, to reduce the amount of soluble species formed during the anodic polarisation of bronze.
4. The open-circuit potential values of bronze samples in non-deoxygenated, non-buffered and buffered SSW over a period of 30 days always less negative in the non-buffered media. After 1-month, the E_{OCP} values in both media seem to converge to −0.131 and −0.155 V, respectively. According to the literature, this potential can be assigned to the formation of cuprite, Cu_2O, and/or nantokite, CuCl.
5. Visual observation of bronze samples with 1-month of exposure in buffered and non-buffered SSW shows a thin film slightly red with white zones and some greenish precipitates (Cu_2O, mixed with SnO_2 and chloride salts i.e. atacamite, paratacamite and/or botalkite).The amounts of greenish corrosion products is higher on the samples immersed in the non-buffered SSW.
6. The SEM images of bronze samples with 1-month exposure in buffered and non-buffered SSW, under open-circuit potential, show significant differences in their morphology: a uniformly cracked surface and a surface with large and spherical precipitates of about 50 μm uniformly distributed, respectively, for bronze in buffered and non-buffered SSW. After the removal of the corrosion products, a pattern that may be assigned to the selective dissolution of Cu, the so-called decuprication process, is well visible, particularly on the coupons that have been immersed in the non-buffered solution of SSW. The size and the density of pits are particularly high on the coupons exposed in the non-buffered SSW.

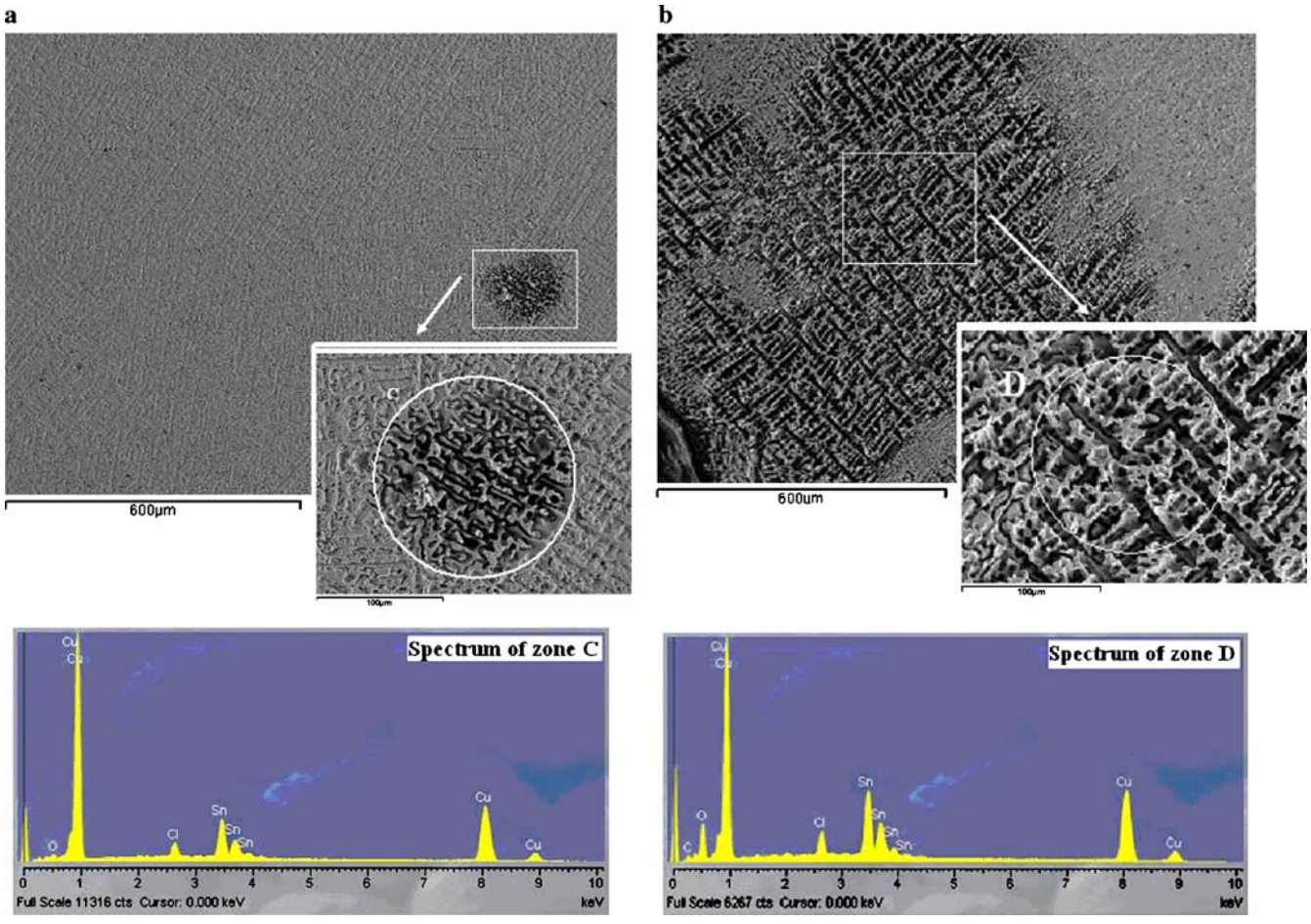

Fig. 10 SEM images and EDS spectra of the surfaces of bronze coupons with 1-month of exposure in **a** buffered, **b** non-buffered SSW solutions

Acknowledgements The authors thank Fundação para Ciência e Tecnologia (FCT) for providing financial support to Centro de Electroquímica e Cinética da Universidade de Lisboa (CECUL) Research Unit POCTI/301/2003 (vertente FEDER) We are grateful to Mrs. Paula Menezes from Laboratório Nacional de Engenharia Civil (LNEC) for all the assistance in the SEM/EDS studies.

References

1. Robbiola L, Blengino JM, Fiaud C (1998) Corros Sci 40:2083
2. Sutter EMM, Millet B, Fiaud C, Linco D (1995) J Electroanal Chem 386:101
3. Chialvo MRG, Marchiano SL, Arvia AJ (1984) J Appl Electrochem 14:165
4. Chialvo MRG, Salvarezza RC, Vazquez Moll D, Arvia AJ (1985) Electrochim Acta 30:501
5. Modestov AD, Zhou D, Wu Y-P, Notoya T, Schweinsberg DP (1995) Corros Sci 36:193
6. Fonseca ITE, Marin ACS, Sá AC (1992) Electrochim Acta 37:2541
7. Fonseca ITE, Sá AIC (1995) In: Ferreira MGS, Simões AMP (eds) Electrochemical methods in corrosion research. Trans Tech Publications, Materials Science Forum, Switzerland, p 511
8. Milosev I, Melikos-Hukovic M, Drogowska M, Ménard H, Brossard L (1992) J Electrochem Soc 139:2409
9. Fonseca ITE, Domingues IMB (1994) Corr Prot Mat 13:24
10. Deslouis C, Tribollet B, Mengoli G, Musiani MM (1988) J Appl Electrochem 18:384
11. Duthil J-P, Mankowski G, Giusti G (1996) Corros Sci 38:1839
12. Edwards M, Rehring J, Meyer T (1994) Corros Sci 50:366
13. Ferreira JP, Rodrigues JA, Fonseca ITE (2004) J Solid State Electrochem 8:260
14. Souto RM, Gonzalez S, Salvarezza RC, Arvia AJ (1994) Electrochim Acta 39:2619
15. Debiemme-Chouvy, Ammeloot F, Sutter EM (2001) J Applied Surf Sci 174:55
16. Ammeloot F, Fiaud C, Sutter EMM (1999) Electrochim Acta 44:2549
17. Mabille I, Bertrand A, Sutter EMM, Fiaud C (2003) Corros Sci 45:855
18. Souissi IN, Bousseimi L, Khosrof S, Triki E (2004) Mater Corros 55:284
19. Mansfeld F, Little B (1992) Electrochim Acta 37:2291
20. ISO/DIS 8407 (1986) Metal and alloys-procedures for the removal of the corrosion products from corrosion tests specimens. Geneve, Switzerland
21. Díaz R, Diéz-Pérez I, Gorostiza P, Sanz F, Morante JR (2003) J Braz Chem Soc 14:523